The Metabolic Fate of Izencitinib, a Gut-selective Pan-JAK Inhibitor, in Humans. Identification of Unusual Fecal Metabolites and Implications for MIST Evaluation.

Suresh Yeola
Biotransformase, Drug Metabolism Consulting, Roswell, GA

Ilaria Badagnani
Theravance Biopharma US Inc

Xiaojun Huang
Theravance Biopharma US Inc

Nathanial L. Segraves
Theravance Biopharma US Inc

Miroslav Rapta
Theravance Biopharma US Inc

Marie T. Borin
Theravance Biopharma US Inc

Glenmar P. Obedencio
Theravance Biopharma US Inc

William L. Fitch
Stanford University School of Medicine

Thomas A. Baillie
University of Washington School of Pharmacy

David L. Bourdet (dbourdet@theravance.com)
Theravance Biopharma US Inc https://orcid.org/0000-0001-6220-1922

Research Article

Keywords: ADME, gut-selective, metabolism, AMS, radiolabel

Posted Date: May 8th, 2023

DOI: https://doi.org/10.21203/rs.3.rs-2815584/v1

Version of Record: A version of this preprint was published at Medicinal Chemistry Research on September 9th, 2023. See the published version at https://doi.org/10.1007/s00044-023-03143-6.

Abstract

Izencitinib is a novel, orally administered pan-JAK inhibitor designed as a gut-selective therapy that was under development for the treatment of inflammatory bowel disease. The objectives of this study were to define the mass balance, routes and rates of excretion, and metabolic fate of izencitinib after oral administration of [^{14}C]-izencitinib in humans. Six healthy adult male subjects were administered a single 100 mg (~ 300 mCi) oral dose of [^{14}C]-izencitinib. Fecal excretion was the dominant route of elimination with > 90% of the administered dose recovered in the feces. Plasma concentrations of total radioactivity and izencitinib were low with the mean terminal half-life of total radioactivity (138 h) exceeding that of izencitinib (32.4 h). Izencitinib represented approximately 17% of the total circulating radioactivity, suggesting the presence of multiple circulating plasma metabolites. However, no metabolites exceeded 10% of total drug-related material in plasma. The major metabolites in feces, M18 and M9, were found to have unusual structures that reflected the presence of a nucleophilic carbon center in the naphthyridine ring of izencitinib. Proposed mechanisms for the formation of these metabolites involved oxidation and rearrangement (M18) and a one-carbon addition, potentially occurring through reaction with endogenous formaldehyde (M9). Given the gut-selective properties of izencitinib, it is proposed that these novel fecal metabolites are the most relevant for evaluating the impact of metabolism on the pharmacological and toxicological properties of izencitinib, and that the circulating plasma metabolite profile is of little consequence in the assessment of the safety characteristics of izencitinib metabolites.

Introduction

Inflammatory bowel disease (IBD) is characterized by chronic inflammation of the gastrointestinal (GI) tract and can manifest as two primary forms: Crohn's disease (CD) and ulcerative colitis (UC) [1–4]. IBD is progressive with patients exhibiting relapsing and remitting episodes and requiring long-term treatment. Several novel and promising pharmacologic interventions have emerged in recent years in IBD such as small molecule inhibitors of Janus kinase (JAK) enzymes [5, 6]. The JAK family, which comprises JAK1-3 and TYK2, has been implicated in the proinflammatory cytokine responses and immune cell activation observed in IBD [7–10]. Tofacitinib (pan-JAK inhibitor [11]) and updacitinib (JAK1 inhibitor [12]) have been approved for the treatment of UC [13–16] and upadacitinib [17] was very recently approved by the Medicines and Healthcare products Regulatory Agency (MHRA) for the treatment of CD. While systemic JAK inhibition is now considered a validated approach in IBD and various other inflammatory diseases, treatment with systemic JAK inhibitors can result in several dose-limiting toxicities, such as hematopoietic abnormalities, opportunistic infections, development of malignancies, and thromboembolic events, which limit the therapeutic benefits of these medicines [8, 18–22]. Evidence that using a gut-selective approach in IBD could result in long-term clinical response while maintaining a favorable safety profile was established with vedolizumab, a novel gut-selective monoclonal antibody administered intravenously, which targets the $\alpha_4\beta_7$ integrin:MAdCAM-1 complex on the surface of memory T cells that migrate predominantly into the GI tract [23–28]. Izencitinib is a novel orally administered pan-JAK inhibitor that was under clinical development for the treatment of IBD. Izencitinib

was designed to be gut-selective, preferentially inhibiting JAK enzymes and the resultant inflammatory response in the gastrointestinal mucosa while minimizing systemic exposure and JAK-dependent safety findings [29–31]. The pharmacokinetics (PK) of orally administered izencitinib was evaluated in healthy volunteers in a first-time-in human (FTIH) study after single and multiple (14 days) ascending doses and in a Phase 1b study in randomized patients with moderately to severely active UC (20, 80 or 270 mg, or placebo for 28 days) [30]. Izencitinib exhibited similarly low plasma exposure in healthy human subjects and in patients with UC and a favorable safety profile. In addition, measured colonic tissue concentrations were in the range sufficient to inhibit JAK/STAT signaling. The PK data in preclinical species and in human subjects support the gut-selective properties designed into izencitinib, including low oral absorption, rapid systemic clearance, and sustained high exposure throughout the GI tract [29–31].

An absorption, distribution, metabolism, and excretion (ADME) study was conducted to confirm the gut-selective disposition of izencitinib in healthy human subjects administered as a single oral dose of [^{14}C]-izencitinib (100 mg, ~ 300 µCi). The study objectives were to assess the routes and rates of elimination of total radioactivity into excreta, and to identify the metabolic profiles in plasma, urine and feces [32–35]. The radiolabeled ADME study conducted with izencitinib highlights several novel and challenging aspects associated with gut-selective agents. As a result of the low oral absorption and extremely low systemic exposures of [^{14}C]-izencitinib, accelerator mass spectrometry (AMS) had to be employed to measure total radioactivity in blood, plasma, and urine, and to profile izencitinib metabolites in plasma and urine. In addition, significant challenges were encountered with structural identification of several atypical metabolites excreted in feces which may reflect exposure of izencitinib to both mammalian enzymes and the gut microbiota. Moreover, the interpretation and application of the FDA and ICH guidance on the safety evaluation of metabolites (generally referred to as metabolites in safety testing or MIST) [36–38], which was originally designed for systemic small molecule therapeutics, required modification in the context of the gut-selective characteristics of izencitinib.

Experimental

Materials

Izencitinib, M1, M6, M9, M10, M11, M12, and M18 were prepared at Theravance Biopharma US Inc. (South San Francisco, CA) or at WuXi AppTec (Hong Kong) Limited, as detailed in the **Supplementary Information** section. [^{14}C]-Izencitinib was synthesized by Vitrax (Placentia, CA), with a specific activity of 57.8 mCi/mmol. The ^{14}C label was in the naphthyridine moiety of izencitinib with 98.9% radiochemical purity.

Study Design and Treatments

This was an open-label, 2-cohort study evaluating the absolute bioavailability, mass balance, PK, excretion, and metabolism of izencitinib in healthy adult male subjects [ClinicalTrials.gov identifier: NCT03408470]. Izencitinib metabolism was evaluated in Cohort 2 only, in which 6 subjects received a single oral dose of 100 mg [^{14}C]-izencitinib (100 mg; ~300 μCi) on Day 1 following an overnight fast.

The trial was conducted at Celerion, Inc. (Lincoln, NE) in accordance with the principles of the International Council on Harmonisation of Technical Requirements for Pharmaceuticals for Human Use, guideline for Good Clinical Practice, and the code of ethics of the World Medical Association's Declaration of Helsinki. The study protocol and conduct were approved by a local institutional review board prior to study initiation. All patients provided written informed consent.

Assessment and Endpoints

Blood, plasma, urine, and feces were collected through the time of subject discharge from the clinical research unit, which occurred once ≥ 90% of the administered radioactive dose had been recovered in excreta by Day 8 or when the subject reached the maximum 15-day stay in the unit. Blood (for whole blood and plasma), urine, and feces were collected to measure total radioactivity, izencitinib concentrations (plasma samples only), and for metabolite profiling (plasma, urine, and feces samples) through at least 168 h (Day 8) post-izencitinib dose. Plasma, urine, and feces were collected for metabolite profiling through at least 168 h (Day 8) post-izencitinib dose. When discharge criteria were not met at Day 8 post-izencitinib dose, the collection of samples continued until discharge criteria were met (blood, urine, and feces samples were collected until 216 h post-izencitinib dose for 1 subject in Cohort 2).

Analytical Methods

Total ^{14}C content (total radioactivity) in urine and feces was measured using liquid scintillation counting (Celerion Inc., Lincoln, NE) or by accelerator mass spectrometry (AMS; Pharmaron, Inc., Germantown, MD) if below the lower limit of quantitation by scintillation counting. All whole blood and plasma samples were measured using AMS (Pharmaron, Inc., Germantown, MD). Liquid chromatography with tandem mass spectrometric detection (Q^2 Solutions, Ithaca, NY) was used to determine the concentrations of izencitinib in plasma and urine.

Metabolite profiles in pooled plasma and urine were determined using high-performance liquid chromatography (HPLC) with fraction collection by AMS (Pharmaron, Inc., Germantown, MD). Technical details for the AMS quantitation methods have been described previously [39]. Metabolite profiles in pooled homogenized feces were determined using HPLC with tandem mass spectrometry (LC-MS/MS) (Theravance Biopharma, South San Francisco).

Metabolite Profiling and Identification in Plasma, Urine, and Feces

Retention times of the metabolite peaks from plasma, urine, and fecal samples were compared with those of metabolites observed in nonclinical (rat and dog) ^{14}C ADME studies (data on file). The structures of the metabolites were determined from non-clinical studies and human fecal samples using HPLC-UV/MS.

Plasma samples were pooled across individual subjects and time points (0–96 h) according to the Hamilton area under the curve (AUC) pooling approach [40]. LC-UV/AMS analyses were conducted using HPLC/UV with offline ^{14}C detection by AMS. For the LC-UV/AMS analysis, 500 µL of plasma from each subject was taken at pre-dose and at various intervals post-dose, resulting in two cross-subject pools. Each cross-subject pooled plasma sample was protein precipitated separately with four volumes of acetonitrile:water (4:1, v/v), vortex mixed and the supernatant was separated. The extraction was repeated two additional times with the resulting supernatant of each extraction combined and concentrated to approximately 300 µL at room temperature. A portion of the concentrated solution was then injected on the HPLC column and fractions were collected.

Urine samples were pooled individually across the 0-168 h total collection interval and subsequently pooled across subjects using a proportional approach based on the ratio of the total weight of the sample excreted at each time point [41]. Urine samples were taken from each collection period from the 0–4 h through the 144–168 h collection intervals and then pooled to generate a single 0-168 h pooled sample for each individual subject. A cross-subject pool was prepared by taking an equal volume from each subject pool and then combining them. The pool represented 95% of the total ^{14}C excreted in the matrix. A portion of the pooled urine was used for AMS fractionation and subsequent AMS analysis.

Fecal samples were pooled individually across time points (0-144 h). An aliquot representing 0.1% (% w/w) of the total fecal homogenate sample was taken from each time interval to make an individual subject pool for up to 0-144 h. Samples were pooled across time points to create a single pooled fecal sample for each subject, ensuring ≥ 89% of the radioactivity was profiled. Pooled fecal homogenate (approximately 1 g) from each subject was extracted with 4.5 mL of acetonitrile. The resulting suspensions were vortexed and centrifuged. The supernatant was separated, and the residue was extracted 2 additional times with 4.5 mL of acetonitrile. The supernatant from the 3 extractions was combined. The combined supernatant from each subject was evaporated to dryness under a stream of nitrogen at room temperature. The dried sample for each subject was then reconstituted in 3.0 mL of 20% acetonitrile in water containing 0.2% formic acid. The resulting suspensions were centrifuged, and supernatants used for radiometric and LC-MS/MS analysis.

Metabolite Profiling in Plasma and Urine

Reference standards [izencitinib; M1 (N-dealkylation of izencitinib); M6 (hydroxylation of izencitinib); M9 (formylation, cyclization and oxidation of izencitinib); M10 (formylation and cyclization of izencitinib); M11 (formylation and dimerization of izencitinib); M12 (hydroxylation of izencitinib); M18 (oxidation of izencitinib)] were added to plasma and urine samples as retention time markers for metabolite profiling

by HPLC. Metabolite peaks were separated on a Phenomenex Synergi Polar RP column (4.6 x 250 mm, 4 µm) at a temperature setpoint of 50ºC. Mobile phase A consisted of 0.2% formic acid in water and mobile phase B consisted of 0.2% formic acid in acetonitrile. The flow rate was 1.0 mL/min, and peaks were separated using a stepwise gradient from 2%-15% mobile phase B over 20 min, held at 15% B for 10 min, 15%-40% B from 30 to 45 min, 40%-50% B from 45 to 50 min, 50%-98% B from 50 to 51 min, 98%-2% B from 51 to 55 min held at 2% B for 5 min before column re-equilibration at 2% B. The total run time was 60 min. The eluent was collected as a series of fractions at 15-sec intervals across each run. Fractions were analyzed either individually or pooled and then analyzed for ^{14}C content by AMS as described earlier. UV chromatograms with the added reference standards were overlaid with the radio-chromatograms based on the AMS detection of fractions and fraction pools to confirm the identity of izencitinib and its metabolites.

Metabolite Profiling in Feces

Chromatographic separation of fecal samples was achieved using a Phenomenex Synergy Polar-RP (4.6 x 250 mm, 4 µm) column with a guard column (Polaris 5 C18-A meta-guard 10 x 2 mm) at a temperature setpoint of 40°C. Mobile phase A was 0.2% formic acid in water; mobile phase B was 0.2% formic acid in acetonitrile. The flow rate was 1.0 mL/min, and peaks were separated using a stepwise gradient from 2%-10% mobile phase B over 12 min, 10%-20% B from 12 to 30 min, 20%-40% B from 30 to 45 min, 40%-50% B from 45 to 50 min, 50%-98% B from 50 to 51 min, back to 2% B at 55 min and held at 2% B for 5 min before column re-equilibration at 2% B. The total run time was 60 min. UV data from a photodiode array (PDA) detector was collected between 200–400 nm.

Metabolite Identification

Radioactive peaks were identified by comparing retention times observed in the radiochromatograms to the retention times in the LC-MS data recorded using Thermo Scientific Software Xcalibur 2.2. Putative metabolites for which the percentage of total radioactivity was 3 times above background were retained and reported as izencitinib metabolites. Major metabolites were considered as those that represented ≥ 10% of total radioactivity in plasma or ≥ 10% of excreted dose in excreta (feces, urine).

Mass spectrometric analyses were carried out on an LTQ Orbitrap XL mass spectrometer equipped with an ESI source with the following parameters: capillary temperature, 300°C; source voltage, 5 kV; sheath gas, 30 (arb) and auxiliary gas, 10 (arb). Four scan events were utilized. Scan 1 captured high resolution full scan (m/z 50-1000) positive ion spectra, with scans 2 and 3 capturing data dependent MS/MS and MS^3 on the most intense ion from scan 1 (MS/MS) and scan 2 (MS^3), respectively. Scan 4 captured data dependent MS^3 on the second most intense ion from scan 2. Collision Induced Dissociation (CID) in the ion trap was conducted with 35% relative collision energy, an isolation width of 4 Da, an activation q of 0.25 and an activation time of 30 ms. For high resolution mass spectra (HRMS) data collection, the full scan resolution was set to 30,000, whereas for HR MS/MS and HR MS^3, the resolution used was 15,000.

The system was calibrated with Thermo Scientific Pierce calibration solutions for mass accuracy. For all metabolites, protonated molecular ions and MS/MS fragment ions exhibited an accurate mass within 5 ppm deviation from the calculated mass.

Synthesis of Metabolites M1, M6, M9, M10, M11, M12 and M18

A total of 7 metabolites of izencitinib were prepared by synthesis to serve as reference materials in the characterization of the corresponding metabolites by LC-MS/MS techniques. Full details of the synthetic procedures are provided in the **Supplementary Information** section. Briefly, the metabolites were prepared as follows: M1 (N-desalkyl metabolite of izencitinib) is the penultimate intermediate in the synthesis of izencitinib whose preparation is described elsewhere (International Patent Publication Number WO 2022/076703). The starting materials used in the synthesis of izencitinib were hydroxylated and the hydroxylated intermediates were used in the preparation of metabolites M6 and M12. Cyclized metabolite M10 was prepared by SEM-protection of the izencitinib pyrazole ring followed by treatment with strong acid. Oxidation of M10 with MnO_2 yielded M9. Dimeric metabolite M11 was prepared by reacting izencitinib with paraformaldehyde at elevated temperature. M18 was prepared by oxidation of izencitinib with oxygen (20 psi) in the presence of azo bis-isobutyronitrile. All synthesized compounds were purified by preparative HPLC and characterized by mass spectrometry or ^{1}H NMR.

Pharmacokinetic Evaluations

Noncompartmental PK parameters were calculated from the total radioactivity of [^{14}C]- izencitinib-derived concentration equivalent-time data in whole blood and plasma as well as plasma izencitinib concentration-time data (Phoenix WinNonlin Version 6.3; Certara USA, Inc., Princeton, NJ).

Mass Balance and Excretion

Urinary excretion was estimated from individual total radioactivity concentration equivalents in urine, or from urinary izencitinib concentrations and volumes using SAS, Version 9.3 (SAS, Institute Inc., Cary, NC). Fecal excretion was estimated from individual total radioactivity concentration equivalents in feces and fecal homogenate weights. Mass balance was calculated individually as the sum of the percent of total radioactivity recovered in urine and feces.

In Vitro Metabolism

The in vitro metabolite profile of [^{14}C]-izencitinib was evaluated in human (mixed gender) liver microsomes. [^{14}C]-Izencitinib (10 μM, 0.06 μCi) was incubated with 1 mg/mL human liver microsomal protein in phosphate buffer pH 7.4 (100 mM) and NADPH (1 mM) for 60 min at 37°C. Time zero samples were withdrawn immediately after addition of compound and served as negative controls. The reactions

were terminated after a 60 min incubation by the addition of an equal volume (200 µL) of ice-cold acetonitrile to the incubation mixture. Samples were centrifuged for 10 min at 5000 x g and the resulting supernatants (75 µL) were analyzed by LC- radio flow detector (Beta-Ram; Lab-Logic, Sheffield, UK) and mass spectrometry (LTQ Orbitrap, Thermo Scientific).

In Vitro Potency

The inhibitory constants (Ki, pKi) of izencitinib and 2 metabolites of interest (M9 and M18) were determined for the human recombinant Janus kinases (JAK) enzymes JAK1, JAK2, JAK3 and TYK2. The ability of each analyte to inhibit the respective JAK enzyme activity was examined using a panel of four LanthaScreen kinase assays that employ a common green fluorescent protein-signal transducer and activator of transcription (GFP-STAT1) fusion protein substrate. IC_{50} values were obtained after analyzing the inhibition curves, and the results were expressed as the negative decadic logarithm, pIC_{50}. Ki values were calculated by the method of Cheng-Prusoff [42] and expressed as negative decadic logarithm, pKi, values.

Results and Discussion

Study Participants

A total of six healthy male subjects were enrolled in Cohort 2 and were dosed on Day 1 with a single oral dose of [^{14}C]-izencitinib (100 mg, 300 µCi). All subjects received study medication and completed the study. The median age was 33 years (age range, 22–52 years), median weight at baseline was 89.9 kg (weight range, 82.5–94.5 kg), and median body mass index was 28.6 kg/m^2 (BMI range, 25.0–31.0 kg/m^2). Three individuals identified as White, 2 individuals as Black or African American, and 1 individual as Native Hawaiian/Pacific Islander/Asian.

Mass Balance and Excretion

After oral administration of [^{14}C]-izencitinib, the majority of total radioactivity was excreted in feces, with most of the radioactive dose excreted within the first 96 h (Fig. 1). After 216 h, the mean (S.D.) total cumulative recovery was 91.0 (12.1)% of the izencitinib radioactive dose, with 91.1 (9.63)% excreted in feces and 0.767 (0.312)% excreted in urine (**Table S1**). Fecal excretion was the dominant route of elimination for izencitinib in humans with > 90% of total radioactivity excreted in the feces after oral administration.

Pharmacokinetics of total radioactivity and izencitinib in plasma

The mean plasma izencitinib concentrations (median t_{max} of 0.783 h) and total radioactivity (median t_{max} of 0.788 h) peaked at a similar time following oral administration of [^{14}C]-izencitinib (**Table S2**). Plasma izencitinib concentrations were lower than those of plasma total radioactivity concentration equivalents but appeared to decline at the same rate (Fig. 2). The peak (C_{max}) and extent of exposure (AUC_{0-t}) to izencitinib averaged 78% and 17%, respectively, of those of total radioactivity, suggesting the presence of circulating metabolites in plasma. The mean apparent terminal $t_{1/2}$ of total plasma radioactivity (138 h) was longer than that of izencitinib (32.4 h). Overall, the systemic plasma exposure was low with maximal izencitinib mean plasma concentrations of ~ 10 ng/mL and rapid elimination. The low systemic exposure combined with the predominantly fecal excretion is consistent with poor oral absorption, and confirmed the expected low plasma levels [i.e., below JAK IC_{50} values] and high local GI concentrations of izencitinib that were observed in the izencitinib first-in-human study [30]. This profile in humans is also consistent with the disposition profile observed in mice where high colonic tissue concentrations were observed with low plasma concentrations [29, 30].

Metabolite Profiling

Metabolites were profiled in pooled plasma, urine, and feces following oral administration of 100 mg [^{14}C]-izencitinib. Representative radiochromatograms in human feces, plasma, and urine, are presented in **Fig. S1** through **S3**, respectively. In plasma, the following metabolites were observed and are summarized in Table 1: M1 (N-dealkylation), M6 (hydroxylation), M9 (formylation, cyclization, and oxidation), M10 (formylation and cyclization), M11 (formylation and dimerization), M12 (hydroxylation), and M18 (oxidation). There were no metabolites circulating in plasma at 10% or greater of the total drug-related exposure. Unchanged izencitinib represented 7.2% of the total circulating radioactivity with the two most abundant metabolites representing 7.8% (M18) and 5.3% (M12) of circulating radioactivity. Several unknown peaks were observed as circulating species, each representing < 10% of the total drug-related exposure.

Table 1
Presence of izencitinib and metabolites in human plasma (% total radioactivity) after oral administration of [^{14}C]-izencitinib

	Biotransformation	Total Circulating Radioactivity (%)
Izencitinib	Parent	7.2
M1	N-Dealkylation	4.3
M6	Hydroxylation	4.0
M9	Formylation, Cyclization and Oxidation	ND
M10	Formylation and Cyclization	3.1
M11	Formylation and Dimerization	2.5
M12	Hydroxylation	5.3
M18	Oxidation	7.8
Data shown represent the % total radioactivity for the cross-subject pooled plasma (AUC_{0-96h})		
Data for unknown peaks were not included; each unknown peak represented < 10% of the total radioactivity		
ND: Not detected in radiochromatogram		

Unchanged izencitinib, M9, and M18 were the major components observed in feces (Table 2). Formation and excretion of M18 and M9 represented a significant fraction of the total administered radioactive dose with fecal excretion of M18 and M9 representing 29% and 23% of the administered dose, respectively. Fecal excretion of izencitinib accounted for an additional 12% of the administered dose.

Table 2
Presence of izencitinib and metabolites (% dose) in human excreta (feces and urine) after oral administration of [^{14}C]-izencitinib

	Biotransformation	% Dose	
		Feces	Urine
Izencitinib	Parent	12	0.1
M1	N-Dealkylation	ND	0.02
M6	Hydroxylation	ND	0.02
M9	Formylation, Cyclization and Oxidation	23	0.07*
M11	Formylation and Dimerization	1.8	
M12	Hydroxylation	ND	0.009
M18	Oxidation	29	0.007
M19	Parent + C_3H_2O	4.1	ND
M28	Oxidation	5.6	ND
Data shown represent the % dose for the mean of the individual fecal homogenate samples that were pooled individually across time points (0-144 h) or the % dose for the cross-subject pooled urine (0-168 h)			
Data for unknown peaks were not included; in feces each unknown peak represented ≤ 5% of the administered dose			
*M9 and M11 were closely eluting metabolites and were observed as a single peak in the respective chromatograms			
ND: Not detected in radiochromatogram			

Limited excretion of total radioactivity (< 1% of the [^{14}C]-izencitinib radioactive dose) was observed in urine; all metabolites and unknown components/chromatographic regions each represented < 0.3% of the administered dose.

Metabolite Identification and Structure Elucidation

Structure determination was performed for nine metabolites of izencitinib, based on their HRMS/MS spectra depicted in the **Supplementary Information** section and on comparison of their HPLC and MS characteristics with those of the corresponding reference materials prepared by synthesis. A summary of the salient details of the HRMS data is presented in Table 3. Proposed metabolic pathways from pooled plasma, urine, and feces are shown in Fig. 3. Particular attention was focused on the identification, and mechanisms of formation, of the major metabolites of izencitinib, namely M9 and M18, and the proposed origins of these metabolites are depicted in Figs. 4 and 5, respectively.

Identification and Proposed Mechanism of Formation of Metabolites M9, M10, M11

The protonated molecular ions of metabolite M9, M10 and M11 were observed at m/z 413.2183, 415.2347 and 409.2355, respectively. The elemental composition of M9, based on the accurate mass of the protonated molecular ion, was found to be $C_{23}H_{25}N_8$, indicating the addition of one carbon and the removal of two hydrogens relative to the structure of izencitinib (elemental composition, $C_{22}H_{27}N_8$). Similarly, the elemental composition of M10 from the accurate mass data was found to be $C_{23}H_{27}N_8$, indicating the addition of one carbon to the elemental composition of izencitinib. Typically, the addition of a one carbon unit is due to methylation, but this possibility was considered unlikely in this case due to elemental composition considerations and the MS/MS fragmentation data for M10. An alternative explanation was reaction of izencitinib with a one carbon electrophile (e.g. formaldehyde) to form M9 and M10. The protonated molecular ion of M11 was at m/z 409.2365, the MS/MS spectrum of which showed major fragment ions at m/z 415 and m/z 403 indicating that the protonated molecular ion m/z 409 was a doubly charged species $(M + 2H)^{++}$. This suggested that M11 was a dimer that may have been formed from an intermediate carbinol in the pathway leading to M10, a minor metabolite in plasma and feces (Fig. 4). While the structure of metabolites M9, M10 and M11 are atypical and unusual in the field of drug metabolism, their formation can be rationalized in terms of the unique electron-rich nature of the C-8 position of the naphthyridine ring system. Thus, it is proposed that M10, a minor metabolite in human plasma, results from addition of a one-carbon unit to the C-8 position of izencitinib and subsequent cyclization onto the N-1 position of the pyrazole ring. Further oxidation of M10 then leads to the major human fecal metabolite M9. The MS/MS fragment ions for M9, M10, and M11 (Table 1) indicated that the modification had occurred on the pyrazole naphthyridine moiety. Additionally, the MS/MS fragmentation pattern and the HPLC retention time for the authentic synthetic standards of M9, M10, and M11 and the biologically derived metabolites were identical, supporting the proposed structures.

The postulated mechanism for the formation of metabolites M9-M11 involving formaldehyde as the source of the one-carbon addition is not without precedent in the area of xenobiotic metabolism. Drug discovery programs have reported the reaction of compounds with endogenous formaldehyde in rats forming novel + 13Da bridged homopiperazine products [43] and during in vitro studies, suggesting that such pathways may be operable in vivo [44]. Endogenous formaldehyde (50 mM) is known to be present in the human body including in the GI tract, liver, and blood[45, 46], suggesting the plausible involvement of this one-carbon unit in the in vivo conversion of izencitinib to metabolites M9 and M10. Further studies will be required to definitively prove the involvement of endogenous formaldehyde as the source of the one-carbon addition in the metabolism of izencitinib.

Identification and Proposed Mechanism of Formation of M18

The protonated molecular ion of metabolite M18 was at m/z 435.2261, corresponding to an elemental composition of $C_{22}H_{27}N_8O_2$, indicating the addition of two oxygen atoms to izencitinib (elemental

composition, $C_{22}H_{27}N_8$). This elemental composition, together with the results of a hydrogen/deuterium exchange experiment (data not shown), suggested that one of the two oxygens in M18 might be in the form of an N-oxide, a conclusion supported by NMR analysis (data not shown). However, attempts to identify M18, by a combination of chemistry (reduction of the putative N-oxide with titanium chloride), MS and NMR techniques, were unsuccessful. Ultimately, X-ray crystallography was used to reveal the structure of this metabolite (**Fig. S4**). M18 was found to be a product formed by oxidation at the C-8 position of izencitinib to give a quinone imine intermediate, hydration of this species, and finally alpha-ketol rearrangement to afford the stable product (Fig. 5). Once again, the structure of this compound reflects the unique electron-rich nature of the C-8 position of the naphthyridine ring system which renders this site susceptible to electrophilic attack.

Identification of Minor Metabolites of Izencitinib

Metabolite M1

The $[M + H]^+$ ion of metabolite M1 (m/z 350) is 53 Da less than that of the parent (m/z 403). The MS/MS fragmentation of M1 showed prominent fragment ions at m/z 283 and 241, which are identical to fragment ions in the CID spectrum of the parent drug, indicating that the modification in M1 has occurred in the bicyclooctane ring of izencitinib. The accurate mass (m/z 350.2088) indicates a structure that lacks the N-cyanoethyl moiety of the parent drug. Therefore, metabolite M1 was assigned as the N-des(cyanoethyl) metabolite of izencitinib.

Metabolite M2:

The full scan mass spectrum of M2 showed prominent ions at m/z 402 ($[M + 2H]^{2+}$) and 803 ($[M + H]^+$), the doubly and singly charged parent ions, respectively. This indicated that metabolite M2 could be a homodimer of izencitinib. The fragment ion m/z 353 indicated the loss of a single methyl pyrazole amine from the dimeric structure of izencitinib. Other fragment ions at m/z 362, 350, 283, 241, 224 and 163 are identical to the fragmentation pattern of the parent drug and support the assignment of M2 as a homodimer of izencitinib. The exact location of the dimer formation in metabolite M2 has not been determined.

Metabolite M3:

The $[M + 2H]^{2+}$ ion at m/z 375 indicated that metabolite M3 could be a heterodimer of izencitinib and its N-des-alkyl metabolite (M1). The fragment ion at 327 was observed after the loss of a single methyl pyrazole amine from the dimer. Another prominent fragment ion at m/z 163 is identical to the bicyclooctane-containing fragment seen in the spectrum of izencitinib, supporting the assignment of M3 as a heterodimer of izencitinib and M1.

Metabolite M6:

Metabolite M6 exhibited an $[M + H]^+$ ion at m/z 419, 16 Da higher than that of the parent drug (m/z 403), which indicates the formation of a hydroxylated metabolite. The MS/MS fragment ions at m/z 366, 299, 257 and 240 are 16 Da higher than those observed in the MS/MS spectrum of izencitinib, while that at m/z 163 did not shift, suggesting that the hydroxylation had occurred on the pyrazole-naphthyridine moiety. The retention time and the MS/MS spectrum of metabolite M6 were identical to those of the synthetic 3-hydroxy izencitinib standard, thereby confirming the structure of M6.

Metabolite M12:

Metabolite M12 exhibited an $[M + H]^+$ ion at m/z 419, 16 Da higher than that of the parent drug (m/z 403), which indicates the formation of a hydroxylated metabolite. Although it was not possible to obtain an MS/MS spectrum of M12 from biological isolates, the accurate mass of the $[M + H]^+$ ion (m/z 419.2309) was within 1 ppm of a synthetic standard of the hydroxymethyl-pyrazole derivative of izencitinib (m/z 419.2302), and the retention time of M12 was identical with that of a synthetic standard, thereby confirming the chemical structure of metabolite M12.

Metabolite M19:

Metabolite M19 exhibited an $[M + H]^+$ ion at m/z 457.2456, 54 Da higher than that of the parent drug (m/z 403.2353; $C_{22}H_{27}N_8$). The elemental composition of metabolite M19 from the accurate mass was found to be $C_{25}H_{29}ON_8$, representing an addition to the izencitinib structure of the elements C_3H_2O. The MS/MS fragment ions at m/z 416, 404, 337 and 295 each appeared at m/z values 54 mass units higher than those observed in the corresponding spectrum of the parent compound (m/z 362, 350, 283, 241). The added C_3H_2O moiety appears to be attached to the pyrazole-naphthyridine moiety of izencitinib to form metabolite M19. The exact structure of M19 could not be determined.

Metabolite M28:

Metabolite M28 exhibited an $[M + H]^+$ ion at m/z 419, 16 Da higher than that of the parent drug (m/z 403). M28 was assigned as an oxidative metabolite of izencitinib, although the lack of an interpretable MS/MS spectrum precluded a specific structural assignment.

In Vitro Metabolism

The metabolism of $[^{14}C]$-izencitinib in vitro was evaluated in human liver microsomes after 60 min incubation (Table 4). Unchanged parent was the major component (54.2% of total radioactivity), while M1 (N-dealkylation) and M2 (homodimer of izencitinib) were the major metabolites representing 20.1% and

10.6% of total radioactivity, respectively. M3 (heterodimer of izencitinib and M1), M11 (formylation and dimerization), and M18 (oxidation) were present as minor metabolites at 5.0%, 3.7%, and 6.5% of total radioactivity, respectively. Lower overall metabolism was observed in human hepatocytes after a 4-h incubation with [^{14}C]-izencitinib; similar metabolites were formed in hepatocytes, with the exception of M2 which was not detected, and M6 (hydroxylation) which was a minor metabolite (2.7% of total radioactivity) in human hepatocytes but was not detected in human liver microsomes (data not shown).

Table 4

Metabolism of [^{14}C]-izencitinib in human liver microsomes (% of total radioactivity)

	Biotransformation	**% Radioactivity**
Izencitinib	Parent	54.2
M1	N-Dealkylation	20.1
M2	Homodimer of izencitinib	10.6
M3	Heterodimer (M1 + izencitinib)	5.0
M11	Formylation and Dimerization	3.7
M18	Oxidation	6.5
[^{14}C]-izencitinib (10 μM, 0.06 μCi) was incubated for 60 min		

The GI-selective design and disposition properties of izencitinib (i.e. > 90% of dose recovered in feces) and the significant portion of the radiolabeled dose recovered as metabolites, raises the question as to the site of metabolic conversion of izencitinib in the body. Other GI-selective agents, such as sulfasalazine, exhibit high levels of fecal excretion while undergoing significant metabolism by intestinal microbiota/bacteria via reductive mechanisms [47, 48]. The major metabolites of izencitinib recovered in feces suggest that greater than 50% of the administered dose was converted to M18 and M9 prior to their excretion in the feces. Given the proposed mechanisms, it is plausible that the formation of M18 and M9 is a reflection of the unique reactivity at the C-8 position of the naphthyridine ring system within the microbiota of the GI tract, thus enabling oxidation to occur as the initial step in the formation of M18 and the direct addition of formaldehyde leading to M9 formation. Exploratory studies in which izencitinib was added to homogenized human feces demonstrated that formation of both M18 and M9 can take place under such conditions (data on file), pointing to the lower GI tract as a possible site of metabolic conversion of izencitinib. However, the in vitro human liver microsomal and hepatocyte incubations also were capable of catalyzing the formation of M18, suggesting that cytochrome P450 enzymes, either in the intestine or the liver, may also be partially responsible for the formation of M18. Additional studies will be required to clarify the sites and enzymes responsible for the formation of these unique metabolites.

In Vitro Potency

Izencitinib is a potent pan-JAK inhibitor with potencies (K_i) at the human recombinant JAK enzymes (JAK1-3 and TYK2) ranging between 0.100 and 1.58 nM [30]. M9 was inactive (K_i >1000 nM) at JAK3 and TYK2 and was a weak inhibitor at JAK1 (K_i of 158 nM) and JAK2 (K_i of 100 nM), with potencies ≥ 500-fold lower than those measured for izencitinib. M18 was inactive (K_i >1000 nM) at all four JAK kinase enzymes. Since M9 and M18 were inactive or were weak pan-JAK inhibitors, even though they were present at approximately 2.0-fold and 2.5-fold higher levels, respectively, relative to izencitinib in human feces (Table 2), neither metabolite is expected to contribute to the pharmacodynamic effects of izencitinib in human GI tissues.

Pharmacological and Toxicological Consequences of Izencitinib Metabolites

The locally-acting nature of a GI-selective agent such as izencitinib raises important questions with respect to the pharmacological and toxicological implications of drug metabolites for such products. Izencitinib was designed to exhibit high colonic concentrations and low systemic exposures in order to maximize its therapeutic effects in the GI tract and minimize systemic safety concerns [29, 30]. The pharmacokinetic profile demonstrated in the Phase 1 program in healthy volunteers, patients with ulcerative colitis, and the current ADME study are consistent with systemic plasma exposures of izencitinib that remain significantly below the JAK IC_{50} for primary pharmacology [30]. All metabolites of izencitinib that were found to be circulating in plasma were present at similar or lower levels than the parent izencitinib, suggesting that they were also unlikely to contribute to systemic JAK-mediated pharmacology. However, it is noteworthy that metabolites M18 and M9 were present in human feces at a level that exceeded those of parent izencitinib by approximately 2-3-fold raising the possibility that these metabolites would have been present at significant levels in the GI-tract and thus capable of mediating pharmacology. Therefore, it was deemed important to test the pharmacological activity of M18 and M9; however, the lack of activity at human recombinant JAK enzymes for M18 and M9, where potencies were ≥ 500-fold lower than those measured for izencitinib, suggested that no metabolites of izencitinib contributed to JAK-mediated pharmacology.

Although the pharmacology of izencitinib metabolites at JAK enzymes proved irrelevant to the overall pharmacological activity of the drug, important questions regarding the toxicological implications of the major fecal metabolites of izencitinib should be addressed. FDA and ICH guidance on the safety evaluation of drug metabolites is contained in the relevant guidance documents commonly referred to as Metabolites in Safety Testing (MIST) [36–38]. Metabolites of interest for purposes of safety evaluation are considered to be those that are ≥ 10% of estimated total drug-related exposure at steady-state. The focus of such evaluation rests on the systemic plasma exposure to the unchanged drug and its metabolites, as determined from a radiolabeled mass balance study such as that reported here. Interestingly, none of the metabolites that were identified in the current study exceeded the 10% threshold

in plasma and thus would not need to be assessed further in the nonclinical toxicology program. However, given the locally-acting and gut-selective nature of izencitinib, we would challenge whether the systemic exposure of drug metabolites is even relevant to toxicology given the poor intestinal absorption and low levels of both izencitinib and total radioactivity observed after oral administration. In fact, izencitinib plasma levels are so low that not even the primary JAK pharmacology is anticipated to be active, much less any toxicological concerns of izencitinib metabolites. Therefore, a focus on systemically circulating metabolites for locally-acting drug products including gut-selective programs (and others such as inhalation, dermal, ocular, etc.) is unlikely to be warranted in most cases given the low systemic exposures for such products. More focus should be placed on metabolites that are present at high concentrations in the local target organ of interest (e.g., GI tract for izencitinib) for further pharmacological and toxicological evaluation.

Conclusion

The mass balance, rates and routes of excretion, and metabolic fate of the novel, gut-selective pan-JAK inhibitor, izencitinib, were evaluated in a human ADME study. Fecal excretion was the dominant route of elimination for izencitinib and, combined with low observed systemic exposure, is consistent with a gut-selective disposition profile in humans. The metabolic pathways of izencitinib were complex and resulted in the formation of metabolites with atypical and unusual structures. Two major metabolites (M18 and M9) were identified in human feces that together represented more than 50% of the administered radiolabeled dose of izencitinib. The proposed mechanisms for the formation of these metabolites involved a highly reactive carbon (C-8 position) that allowed for the oxidation and rearrangement of izencitinib resulting in the formation of a rearrangement product (M18) and a proposed one-carbon addition with formaldehyde that resulted in the formation of a tetracyclic product (M9). Metabolites M18 and M9 did not retain pharmacological activity at the JAK isozymes (JAK 1–3 and TYK2). Given the high levels of these metabolites observed in feces and the gut-selective disposition of izencitinib, the pharmacological and toxicological implications of izencitinib metabolism should center around the metabolism observed in the GI tract and resulting excretion in feces, as opposed to the low-level metabolites that are circulating in human plasma. This work has implications for the metabolic evaluation of locally-acting drug products (e.g., gut-selective, inhaled, dermal, ocular) that exhibit high local tissue concentrations and low systemic exposures and which do not conform to the focus of the current MIST guidance on the safety evaluation of drug metabolites.

Abbreviations

ADME, absorption, distribution, metabolism, and excretion

AMS, accelerator mass spectrometry

AUC, area under the curve

$AUC_{0\text{-}96h}$, area under the curve from time zero to 96 hours

$AUC_{0\text{-}t}$, area under the curve from time zero to the last measured concentration

CID, collision induced dissociation

C_{max}, maximum concentration

CD, Crohn's disease

FTIH, first-time-in human

GFP-STAT1, green fluorescent protein-signal transducer and activator of transcription

GI, gastrointestinal

h, hour or hours

HLM, human liver microsomes

HPLC, high-performance liquid chromatography

HPLC-UV/MS, HPLC coupled with mass spectrometry and ultraviolet detection

HRMS, high resolution mass spectra
IBD, inflammatory bowel disease

IC_{50}, half maximal inhibitory concentration

JAK, Janus kinase

Ki, dissociation constant

LC-MS/MS, HPLC with tandem mass spectrometry

LC-UV/AMS

MHRA Medicines and Healthcare products Regulatory Agency

MIST, metabolites in safety testing

MS^3, third generation product ions mass spectrometry

ND, not detected

^1H NMR; NMR, nuclear magnetic resonance

PDA, photodiode array

pIC_{50}, negative log of IC_{50}

pKi, negative log of Ki

PK, pharmacokinetics

RP, reverse phase

$t_{1/2}$, half life

T_{max}, time of maximum concentration

S.D., standard deviation

SEM, standard error of the mean

UC, ulcerative colitis

UV, ultraviolet

Declarations

Author Information

Acknowledgments

The authors and Theravance Biopharma thank the subjects for their participation in the clinical trial, and the principal investigator and clinical site staff at Celerion, Inc. in Lincoln, Nebraska. The study was funded by Theravance Biopharma Ireland Limited.

Conflicts of interest

IB, **GO, MR**, and **DLB** are employees of Theravance Biopharma US, Inc., and shareholders in Theravance Biopharma, Inc. **MTB**, **WLF**, **TAB** are paid consultants for Theravance Biopharma US, Inc. **SY**, **NLS**, and **XH** are former employees of Theravance Biopharma US, Inc., and may hold shares in Theravance Biopharma, Inc.

References

1. Sobczak M, Fabisiak A, Murawska N, Wesolowska E, Wierzbicka P, Wlazlowski M et al (2014) Current overview of extrinsic and intrinsic factors in etiology and progression of inflammatory bowel diseases. Pharmacol Rep 66(5):766–775. 10.1016/j.pharep.2014.04.005

2. Segal JP, LeBlanc JF, Hart AL (2021) Ulcerative colitis: an update. Clin Med (Lond) 21(2):135–139. 10.7861/clinmed.2021-0080
3. Du L, Ha C (2020) Epidemiology and Pathogenesis of Ulcerative Colitis. Gastroenterol Clin North Am 49(4):643–654. 10.1016/j.gtc.2020.07.005
4. Petagna L, Antonelli A, Ganini C, Bellato V, Campanelli M, Divizia A et al (2020) Pathophysiology of Crohn's disease inflammation and recurrence. Biol Direct 15(1):23. 10.1186/s13062-020-00280-5
5. Al-Bawardy B, Shivashankar R, Proctor DD (2021) Novel and Emerging Therapies for Inflammatory Bowel Disease. Front Pharmacol 12:651415. 10.3389/fphar.2021.651415
6. Santiago M, Stocker F, Ministro P, Goncalves R, Carvalho D, Portela F et al (2022) Incidence Trends of Inflammatory Bowel Disease in a Southern European Country: A Mirror of the Western World? Clin Transl Gastroenterol 13(5):e00481. 10.14309/ctg.0000000000000481
7. Boland BS, Sandborn WJ, Chang JT (2014) Update on Janus kinase antagonists in inflammatory bowel disease. Gastroenterol Clin North Am 43(3):603–617. 10.1016/j.gtc.2014.05.011
8. Dudek P, Fabisiak A, Zatorski H, Malecka-Wojciesko E, Talar-Wojnarowska R, Efficacy (2021) Safety and Future Perspectives of JAK Inhibitors in the IBD Treatment. J Clin Med 10(23). 10.3390/jcm10235660
9. Harris C, Cummings JRF (2021) JAK1 inhibition and inflammatory bowel disease. Rheumatology (Oxford) 60(Supple 2):ii45–ii51. 10.1093/rheumatology/keaa896
10. Cordes F, Foell D, Ding JN, Varga G, Bettenworth D (2020) Differential regulation of JAK/STAT-signaling in patients with ulcerative colitis and Crohn's disease. World J Gastroenterol 26(28):4055–4075. 10.3748/wjg.v26.i28.4055
11. Meyer DM, Jesson MI, Li X, Elrick MM, Funckes-Shippy CL, Warner JD et al (2010) Anti-inflammatory activity and neutrophil reductions mediated by the JAK1/JAK3 inhibitor, CP-690,550, in rat adjuvant-induced arthritis. J Inflamm (Lond) 7:41. 10.1186/1476-9255-7-41
12. Parmentier JM, Voss J, Graff C, Schwartz A, Argiriadi M, Friedman M et al (2018) In vitro and in vivo characterization of the JAK1 selectivity of upadacitinib (ABT-494). BMC Rheumatol 2:23. 10.1186/s41927-018-0031-x
13. FDA, Xeljanz Prescribing I (2018) https://www.accessdata.fda.gov/drugsatfda_docs/label/2018/203214s018lbl.pdf
14. EMA. Xeljanz Summary of Product Characteristics (2018) https://www.ema.europa.eu/en/documents/product-information/xeljanz-epar-product-information_en.pdf
15. FDA, Rinvoq Prescribing I (2022) https://www.accessdata.fda.gov/drugsatfda_docs/label/2022/211675s007lbl.pdf
16. EMA. Rinvoq Summary of Product Characteristics (2022) https://www.ema.europa.eu/en/documents/product-information/rinvoq-epar-product-information_en.pdf

17. MHRA. Rinvoq Summary of Product Characteristics (2023) https://www.medicines.org.uk/emc/product/10972/smpc/print
18. Agrawal M, Kim ES, Colombel JF (2020) JAK Inhibitors Safety in Ulcerative Colitis: Practical Implications. J Crohns Colitis 14(Supplement2):S755–S60. 10.1093/ecco-jcc/jjaa017
19. Sandborn WJ, Su C, Sands BE, D'Haens GR, Vermeire S, Schreiber S et al (2017) Tofacitinib as Induction and Maintenance Therapy for Ulcerative Colitis. N Engl J Med 376(18):1723–1736. 10.1056/NEJMoa1606910
20. Sandborn WJ, Panes J, Sands BE, Reinisch W, Su C, Lawendy N et al (2019) Venous thromboembolic events in the tofacitinib ulcerative colitis clinical development programme. Aliment Pharmacol Ther 50(10):1068–1076. 10.1111/apt.15514
21. Sandborn WJ, Feagan BG, Loftus EV Jr, Peyrin-Biroulet L, Van Assche G, D'Haens G et al (2020) Efficacy and Safety of Upadacitinib in a Randomized Trial of Patients With Crohn's Disease. Gastroenterology 158(8):2123–38e8. 10.1053/j.gastro.2020.01.047
22. Sandborn WJ, Ghosh S, Panes J, Schreiber S, D'Haens G, Tanida S et al (2020) Efficacy of Upadacitinib in a Randomized Trial of Patients With Active Ulcerative Colitis. Gastroenterology 158(8):2139–49e14. 10.1053/j.gastro.2020.02.030
23. Wyant T, Fedyk E, Abhyankar B (2016) An Overview of the Mechanism of Action of the Monoclonal Antibody Vedolizumab. J Crohns Colitis 10(12):1437–1444. 10.1093/ecco-jcc/jjw092
24. Colombel JF, Sands BE, Rutgeerts P, Sandborn W, Danese S, D'Haens G et al (2017) The safety of vedolizumab for ulcerative colitis and Crohn's disease. Gut 66(5):839–851. 10.1136/gutjnl-2015-311079
25. Lukin D, Faleck D, Xu R, Zhang Y, Weiss A, Aniwan S et al (2022) Comparative Safety and Effectiveness of Vedolizumab to Tumor Necrosis Factor Antagonist Therapy for Ulcerative Colitis. Clin Gastroenterol Hepatol 20(1):126–135. 10.1016/j.cgh.2020.10.003
26. Loftus EV Jr, Colombel JF, Feagan BG, Vermeire S, Sandborn WJ, Sands BE et al (2017) Long-term Efficacy of Vedolizumab for Ulcerative Colitis. J Crohns Colitis 11(4):400–411. 10.1093/ecco-jcc/jjw177
27. Loftus EV Jr, Feagan BG, Panaccione R, Colombel JF, Sandborn WJ, Sands BE et al (2020) Long-term safety of vedolizumab for inflammatory bowel disease. Aliment Pharmacol Ther 52(8):1353–1365. 10.1111/apt.16060
28. Vermeire S, Loftus EV Jr, Colombel JF, Feagan BG, Sandborn WJ, Sands BE et al (2017) Long-term Efficacy of Vedolizumab for Crohn's Disease. J Crohns Colitis 11(4):412–424. 10.1093/ecco-jcc/jjw176
29. Beattie DT, Pulido-Rios MT, Shen F, Ho M, Situ E, Tsuruda PR et al (2017) Intestinally-restricted Janus Kinase inhibition: a potential approach to maximize the therapeutic index in inflammatory bowel disease therapy. J Inflamm (Lond) 14:28. 10.1186/s12950-017-0175-2
30. Sandborn WJ, Nguyen DD, Beattie DT, Brassil P, Krey W, Woo J et al (2020) Development of Gut-Selective Pan-Janus Kinase Inhibitor TD-1473 for Ulcerative Colitis: A Translational Medicine

Programme. J Crohns Colitis 14(9):1202–1213. 10.1093/ecco-jcc/jjaa049

31. Hardwick RN, Brassil P, Badagnani I, Perkins K, Obedencio GP, Kim AS et al (2022) Gut-Selective Design of Orally Administered Izencitinib (TD-1473) Limits Systemic Exposure and Effects of Janus Kinase Inhibition in Nonclinical Species. Toxicol Sci 186(2):323–337. 10.1093/toxsci/kfac002
32. Penner N, Xu L, Prakash C (2012) Radiolabeled absorption, distribution, metabolism, and excretion studies in drug development: why, when, and how? Chem Res Toxicol 25(3):513–531. 10.1021/tx300050f
33. Spracklin DK, Chen D, Bergman AJ, Callegari E, Obach RS (2020) Mini-Review: Comprehensive Drug Disposition Knowledge Generated in the Modern Human Radiolabeled ADME Study. CPT Pharmacometrics Syst Pharmacol 9(8):428–434. 10.1002/psp4.12540
34. Young GC, Spracklin DK, James AD, Hvenegaard MG, Scarfe G, Wagner DS et al (2022) Considerations for Human ADME Strategy and Design Paradigm Shift(s) - An Industry White Paper. Clin Pharmacol Ther. 10.1002/cpt.2691
35. FDA. Clinical Pharmacology Considerations for Human Radiolabeled Mass Balance Studies (Draft) (2022) https://www.fda.gov/regulatory-information/search-fda-guidance-documents/clinical-pharmacology-considerations-human-radiolabeled-mass-balance-studies
36. FDA. Safety Testing of Drug Metabolites Guidance for Industry (2020) https://www.fda.gov/media/72279/download
37. ICH. ICH M3(R2 (2010) Guidance for industry: nonclinical safety studies for the conduct of human clinical trials and marketing authorization for pharmaceuticals. https://www.fda.gov/media/71542/download
38. ICH. ICH Guideline M12 on drug interaction studies (Step 2b, Draft) (2022) https://www.ema.europa.eu/en/documents/scientific-guideline/draft-ich-guideline-m12-drug-interaction-studies-step-2b_en.pdf
39. Bourdet DL, Yeola S, Hegde SS, Colson PJ, Barnes CN, Borin MT (2020) Revefenacin Absorption, Metabolism, and Excretion in Healthy Subjects and Pharmacological Activity of Its Major Metabolite. Drug Metab Dispos 48(12):1312–1320. 10.1124/dmd.120.000103
40. Hamilton RA, Garnett WR, Kline BJ (1981) Determination of mean valproic acid serum level by assay of a single pooled sample. Clin Pharmacol Ther 29(3):408–413. 10.1038/clpt.1981.56
41. Penner N, Klunk LJ, Prakash C (2009) Human radiolabeled mass balance studies: objectives, utilities and limitations. Biopharm Drug Dispos 30(4):185–203. 10.1002/bdd.661
42. Cheng Y, Prusoff WH (1973) Relationship between the inhibition constant (K1) and the concentration of inhibitor which causes 50 per cent inhibition (I50) of an enzymatic reaction. Biochem Pharmacol 22(23):3099–3108. 10.1016/0006-2952(73)90196-2
43. Martin S, Lenz EM, Temesi D, Wild M, Clench MR (2012) Reaction of homopiperazine with endogenous formaldehyde: a carbon hydrogen addition metabolite/product identified in rat urine and blood. Drug Metab Dispos 40(8):1478–1486. 10.1124/dmd.112.044917

44. Zhang M, Resuello CM, Guo J, Powell ME, Elmore CS, Hu J et al (2013) Contribution of artifacts to N-methylated piperazine cyanide adduct formation in vitro from N-alkyl piperazine analogs. Drug Metab Dispos 41(5):1023–1034. 10.1124/dmd.112.050450
45. Wei Y, Wang M, Liu H, Niu Y, Wang S, Zhang F et al (2019) Simultaneous determination of seven endogenous aldehydes in human blood by headspace gas chromatography-mass spectrometry. J Chromatogr B Analyt Technol Biomed Life Sci 1118–1119:85–92. 10.1016/j.jchromb.2019.04.027
46. Luo W, Li H, Zhang Y, Ang CY (2001) Determination of formaldehyde in blood plasma by high-performance liquid chromatography with fluorescence detection. J Chromatogr B Biomed Sci Appl 753(2):253–257. 10.1016/s0378-4347(00)00552-1
47. Peppercorn MA (1984) Sulfasalazine. Pharmacology, clinical use, toxicity, and related new drug development. Ann Intern Med 101(3):377–386. 10.7326/0003-4819-101-3-377
48. Wilson ID, Nicholson JK (2017) Gut microbiome interactions with drug metabolism, efficacy, and toxicity. Transl Res 179:204–222. 10.1016/j.trsl.2016.08.002

Tables

Table 3 is available in the Supplementary Files section.

Figures

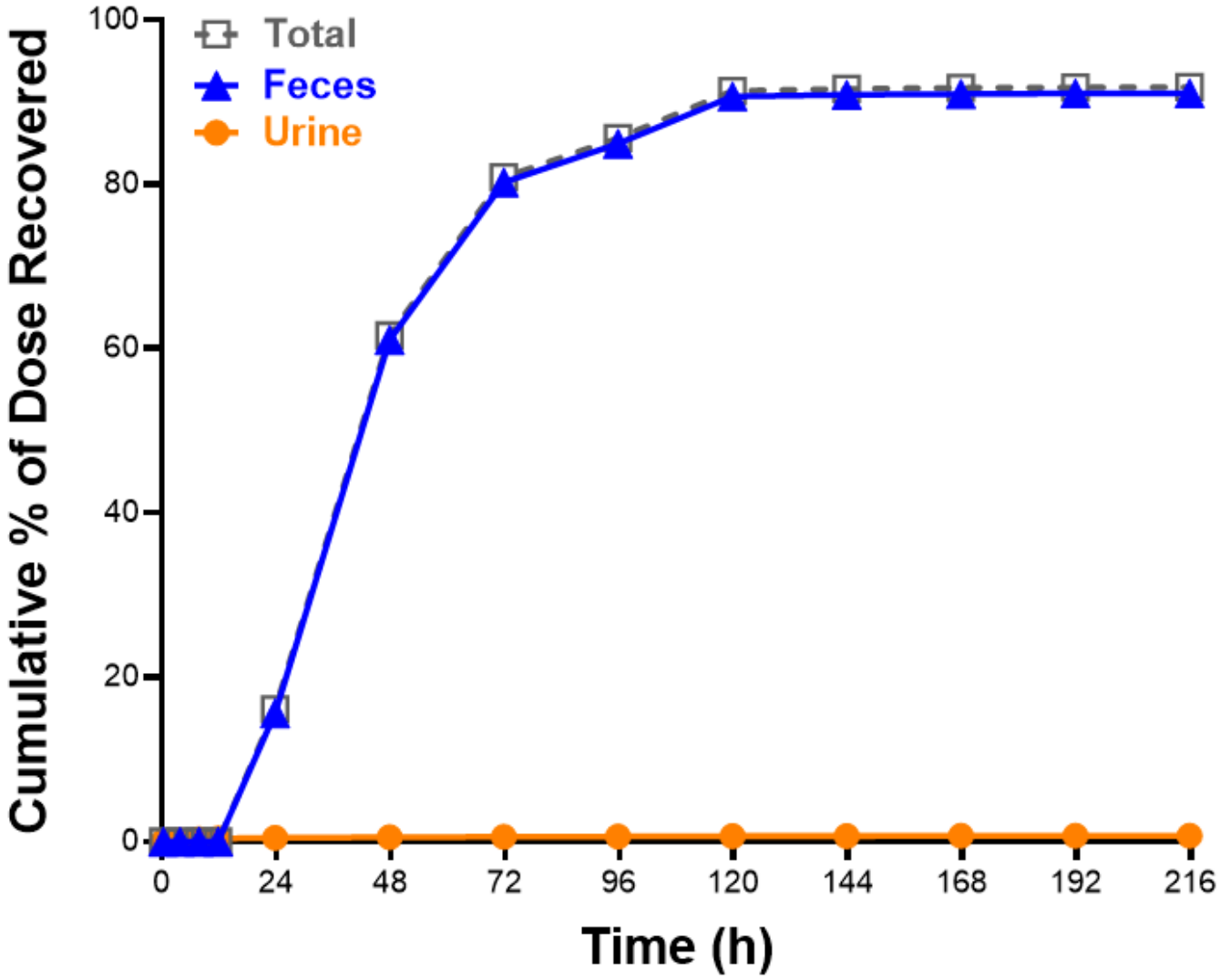

Figure 1

Mean cumulative recovery of total radioactivity (% of dose) in human excreta after oral administration of [^{14}C]-izencitinib, 100 mg (n=6)

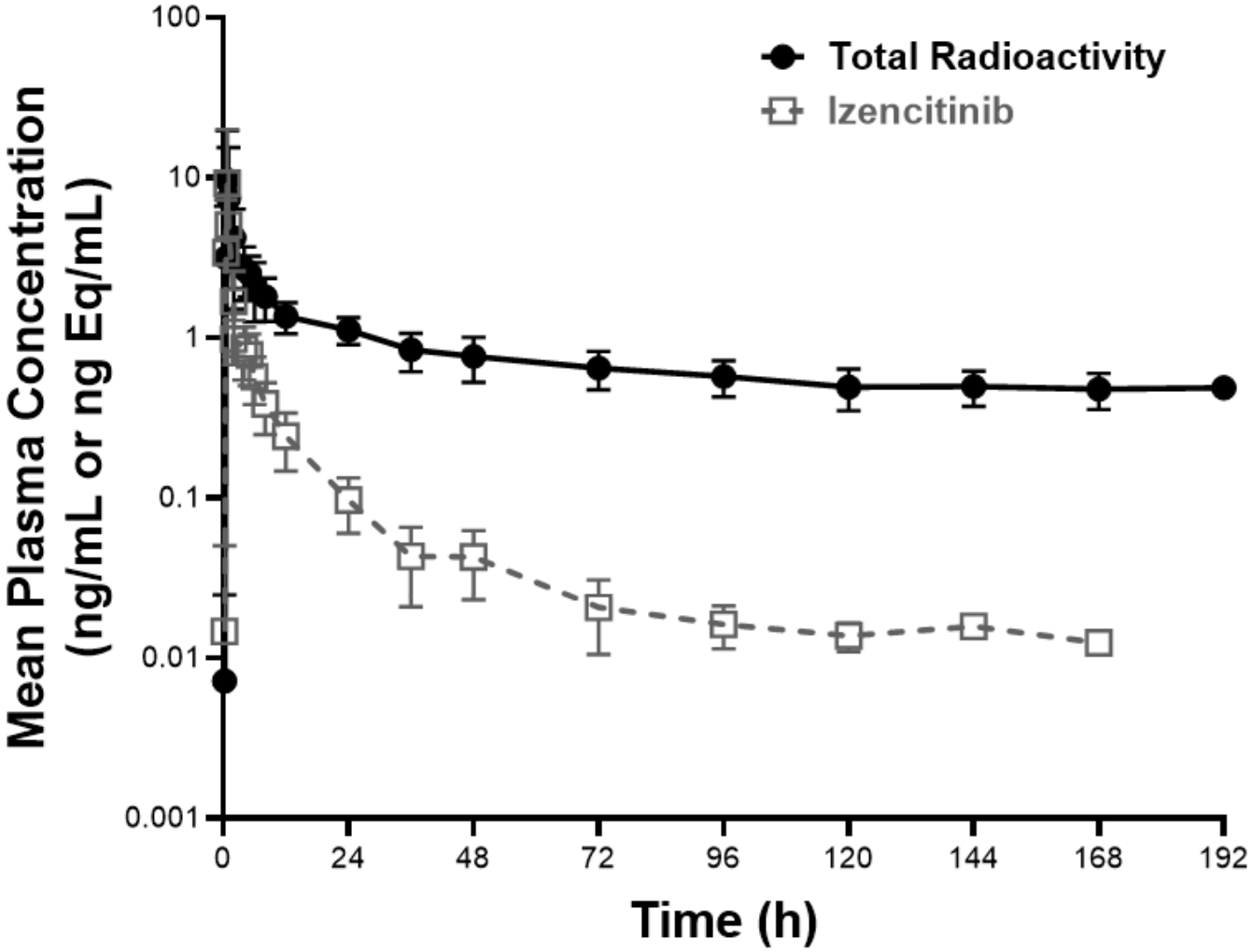

Figure 2

Mean (standard deviation) plasma concentration-time profiles of izencitinib and total radioactivity in male subjects administered a single oral dose of [^{14}C]-izencitinib, 100 mg (n=6)

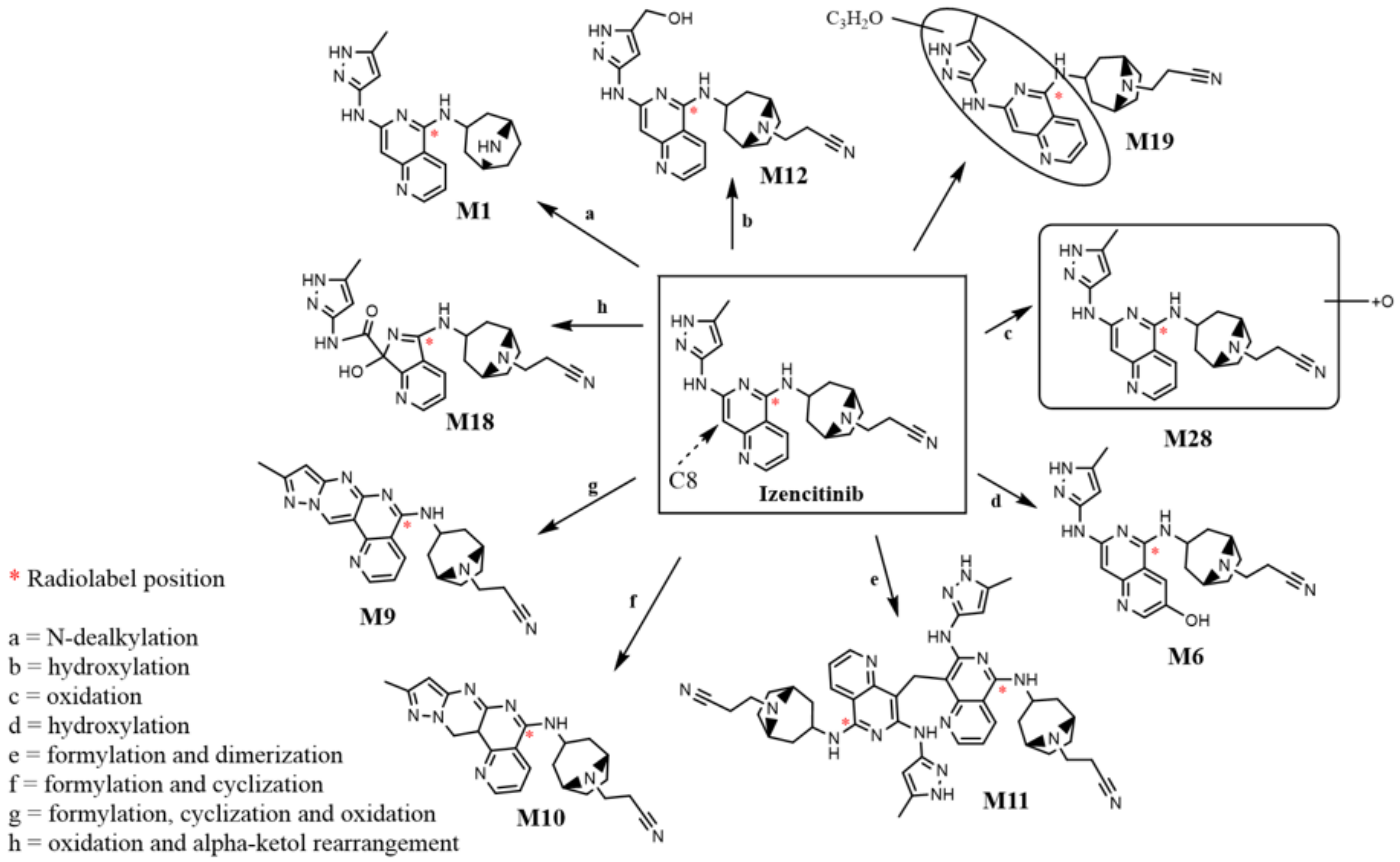

Figure 3

Primary metabolic pathways of izencitinib in humans

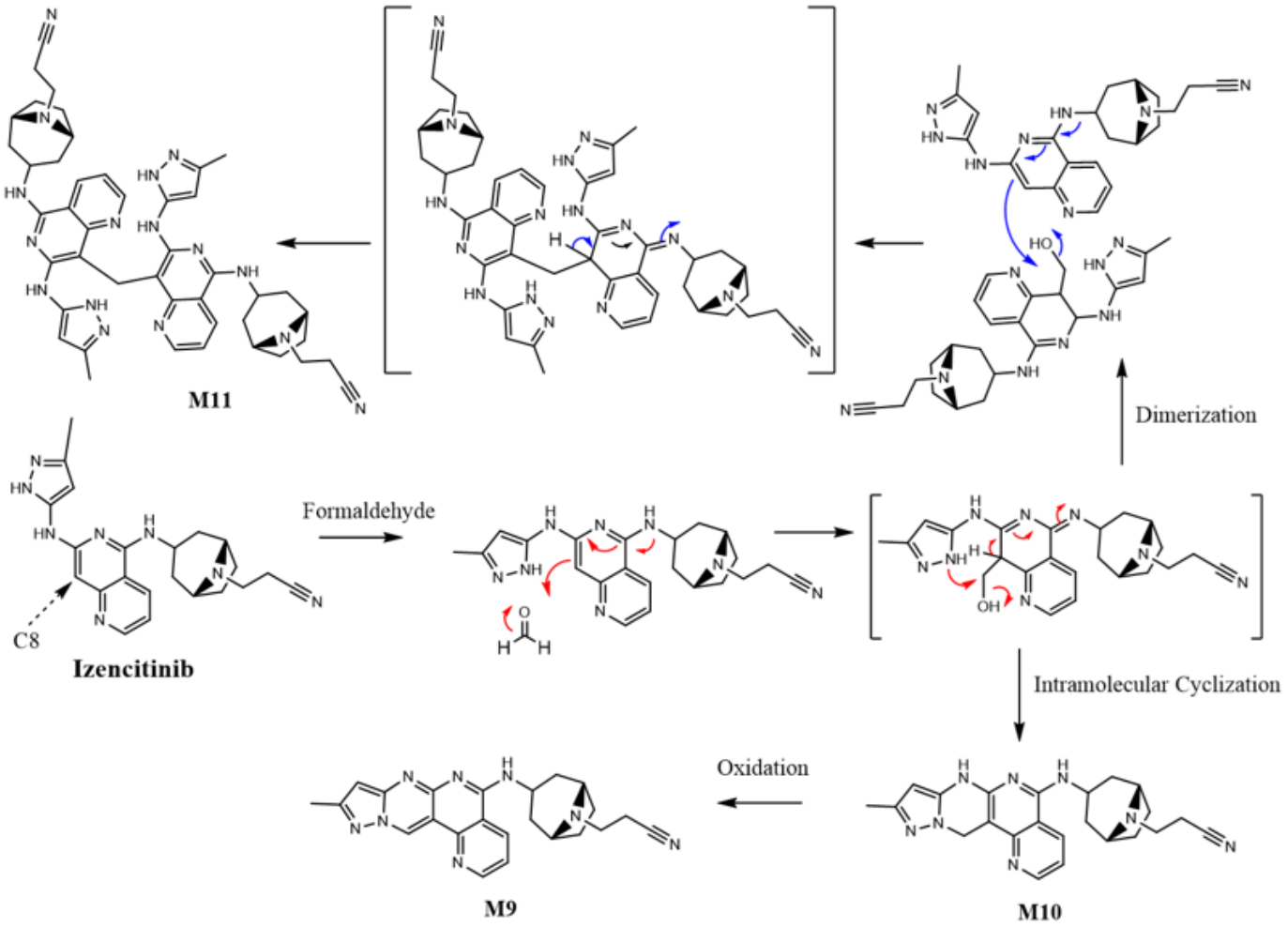

Figure 4

Proposed mechanism of M9, M10 and M11 formation from izencitinib

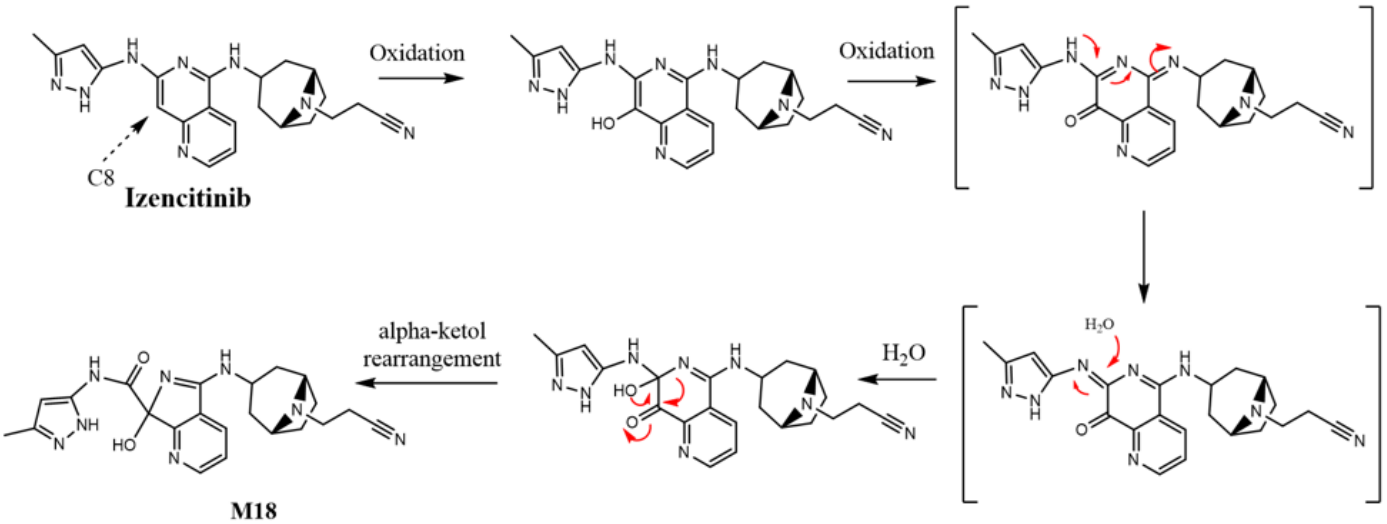

Figure 5

Proposed mechanism of formation of M18 from izencitinib

Supplementary Files

This is a list of supplementary files associated with this preprint. Click to download.

- Table3.docx
- GraphicalAbstract.png
- IzencitinibMetabolismMedChemResSupInfoFin.pdf